

Supporting Information

Balancing the Interplay Between Ligand Ejection and Therapeutic Window Light Absorption in Ruthenium Polypyridyl Complexes

Annie M. McCullough^{†#}, Jiaqi Chen^{§#}, Nathaniel P. Valentine[†], Toney M. Franklin[†], Andrew P. Cantrell[†], Vayda M. Darnell[†], Qasim Qureshi[‡], Kenneth Hanson[§], Steven M. Shell[‡], Dennis L. Ashford^{*,†}

[†]Department of Natural Sciences, Tusculum University, Greeneville, Tennessee 37745, United States

[§]Department of Chemistry & Biochemistry, Florida State University, Tallahassee, Florida 32306, United States

[‡]Department of Natural Sciences, University of Virginia College at Wise, Wise, Virginia, 24293, United States

#Authors contributed equally

Contents

1) Instrumentation	S2
2) Synthesis and NMR spectra	S2-7
3) Figure S1. Cyclic voltammograms of 1-5	S8
4) Figure S2. Electrochemical potentials for 1-5	S9
5) Figure S3. Photolysis Setup	S9
6) Figure S4. Photolysis experiments with 467 nm lamp	S10
7) Figure S5. Photolysis experiments with white lamp	S11
8) Table S1. Molar absorptivity and light intensity for photolysis	S12
9) Figure S5. Long term stability spectra	S12
10) Figure S6. Absorption spectra of [Ru(bpy) ₂ (6,6'-dmb)] ²⁺ during photolysis	S13
11) Figure S7. Normalized emission spectra of 1-5	S13
12) Figure S8. Relative emission intensity for 4 and 5	S14
13) Figure S9. Temperature dependent emission decays for 1	S14
14) Figure S10. Temperature dependent emission decays for 2	S15

15) Figure S11. Temperature dependent emission decays for 3	S15
14) Figure S12. MTT assays of complexes 1-5	S16
15) Figure S13. Percent change in cell viability in light and dark.....	S16
16) Figure S14. MTT assays of cisplatin and $[\text{Ru}(\text{bpy})_2(6,6'\text{-dmb})]^{2+}$	S17

Experimental Section

Instrumentation

Electrochemical Measurements. Electrochemistry was completed using a Gamry Instruments 1010E potentiostat with a glassy carbon working electrode, graphite counter electrode, and a Ag/AgNO₃ reference electrode (0.01 M AgNO₃/0.1 M tetra-n-butylammonium hexafluorophosphate (TBAPF₆) supporting electrolyte in dry CH₃CN, standardized with Ru(bpy)₃²⁺ redox couple at 1.29 V vs SCE).¹⁻⁴ E_{1/2} values were obtained from the peak currents in square wave voltammograms. Reductive electrochemistry was carried out in dry, deaerated CH₃CN with 0.1 M TBAPF₆ as the supporting electrolyte under an atmosphere of nitrogen.

UV-Vis Absorption Spectra. UV-vis absorption spectra were recorded on an Agilent Technologies Cary 60 UV-Vis spectrometer. Extinction coefficients for the complexes in H₂O were determined from the absorption spectra of solutions having known concentrations of the complex.

Steady-State and Time-Resolved Emission. Emission data were collected using an Edinburgh FLS980 spectrometer. For steady-state emission samples were excited using light output from a housed 450 W Xe lamp passed through a single grating (1800 l/mm, 250 nm blaze) Czerny-Turner monochromator. Emission from the sample was first passed through a 475 nm long-pass color filter, then a single grating (1800 l/mm, 500 nm blaze) Czerny-Turner monochromator and finally detected by a peltier-cooled Hamamatsu R928 photomultiplier tube. Time-resolved emission were acquired using the time-correlated single-photon counting capability (1024 channels; 100 ns window) with excitation provided by an Edinburgh EPL-405 ps pulsed light emitting diode (405 ± 10 nm, pulse width 57.6 ps) operated at 10 MHz. Emission was passed through a 420 nm long-pass filter and detected as described above. Emission decays were fit with a mono-exponential function ($y = A_1e^{-k_1x} + y_0$) using Edinburgh software package. The temperature was varied using at PolyScience 9101 digital temperature controller and bath filled with ethylene glycol and water circulated through the Edinburgh FLS980 cuvette mount.

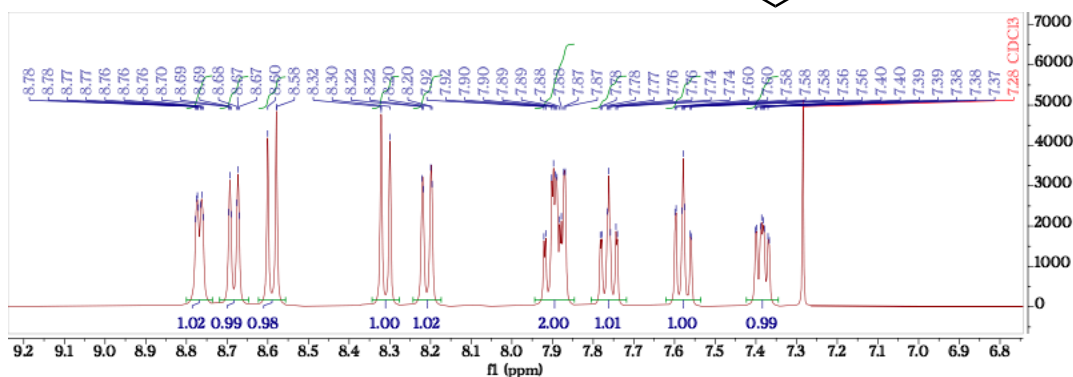
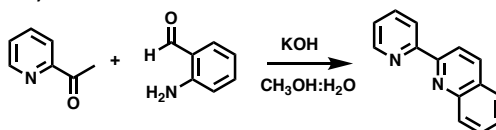
Photolysis. Ligand ejection studies were completed using the apparatus shown in Figure S3. The light from a Kessil PR160 (467 nm, 120 mW/cm² at 5 cm) or a GLORIOUS-LITE 30W LED (240W halogen equivalent), 3000 LM broad spectrum white flood lamp was illuminated onto a quartz cuvette containing 3 mL of the solutions of interest 5 cm away from the light source. The absorption spectrum of the sample was monitored on an Agilent Technologies Cary 60 UV-vis spectrometer at specific time intervals to monitor photoinduced ligand ejection. The samples were irradiated at varying lamp intensities to compensate for differing absorptivities at 467 nm (25% for **1**, 25% for **2**, 75% for **3**, 100% for **4**, and 75% for **5**) when the Kessil lamp was used.

Cell Assays. Cell viability was monitored via an MTT assay as previously reported.^{5,6} HEK293T cells were cultured in 1x D-MEM (Gibco) supplemented with 10% fetal bovine serum (Gibco). Cultures were incubated under standard growth conditions at 37 °C, 5% CO₂. Cells were seeded in to 96-well plates at a density of 20,000 cells/mL and allowed to adhere overnight. Complete growth medium was then supplemented with either DMSO solvent (mock treatment) or increasing concentrations of complexes and incubated for 48 hours at 37 °C. In order to test the effects of photolysis, cultures either exposed to or covered from irradiation *in situ* after compound addition. The samples were irradiated with a Kessil PR160 (467 nm, 120 mW/cm² at 5 cm) lamp at 10 cm from the top of microtiter plate at 25% lamp intensity for 60 minutes. 25% lamp intensity was selected to limit thermal buildup of the cell samples. Irradiation occurred either immediately (no pre-incubation) or 60 minutes (pre-incubation) after addition of the compounds. Following incubation, MTT dye solution (5 g/L in 1x PBS) was added to cultures at a 1:10 dilution and incubated for 4 hours under standard growth conditions. An equal volume of Solubilization Buffer [40% (v/v) DMF, 26% (w/v) SDS, 2% (v/v) acetic acid, pH 4.7] was added and incubated under standard conditions for 10 minutes. Absorbance was measured at λ570 nm using a BioTek Cytation1 Multi-Mode plate reader. Cell viability was measured as a percentage in dye response in complex-treated cultures compared to the mock-treated cultures.

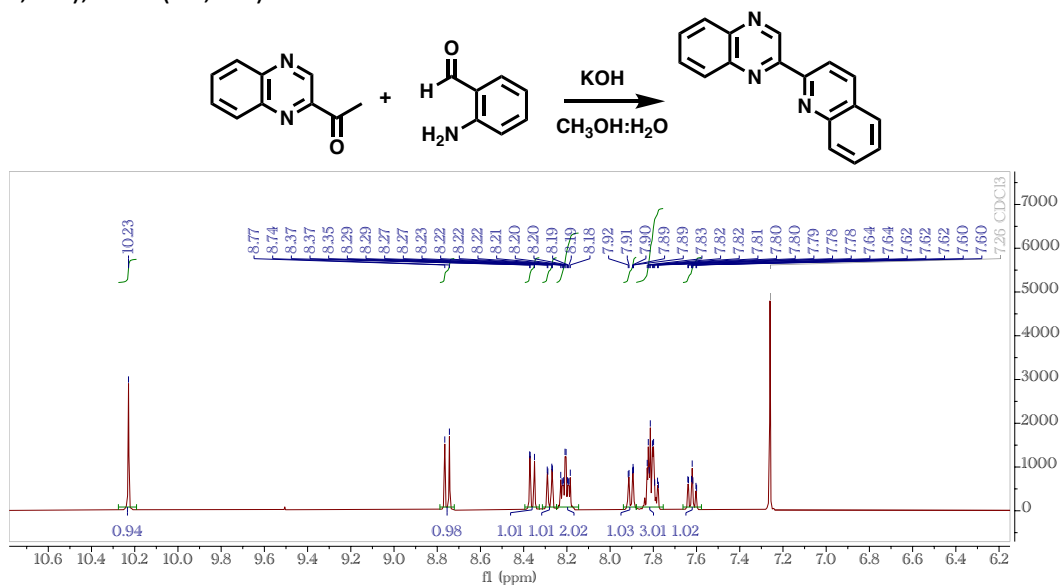
Synthesis

2,2'-bipyridine (**bpy**, **L1**) and 2,2'-biquinoline (**L3**) were purchased from Fischer Scientific and used without further purification. The starting material *cis*-[Ru(**bpy**)₂Cl₂] was synthesized as previously reported.⁷

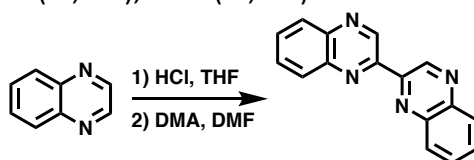
2-(pyridine-2-yl)quinoline (**L2**). 2-acetylpyridine (0.30 g, 2.48 mmol) and 2-aminobenzaldehyde (0.30 g, 2.48 mmol) were dissolved in 15 mL of 1:1 CH₃OH:H₂O. To the solution was added KOH (0.277 g, 4.94 mmol) and the solution was stirred at 60°C for 12 hours. The reaction was quenched by the addition of 30 mL of water and the precipitate was collected and allowed to air dry (0.49 g, 96 %) . This product was used without further purification. ¹H NMR (400 MHz, CDCl₃): δ 8.76 (d, 1H), 8.68 (d, 1H), 8.59 (d, 1H), 8.31 (d, 1H), 8.20 (d, 1H), 7.89 (m, 2H), 7.76 (dd, 1H), 7.57 (dd, 1H), 7.38 (dd, 1H).

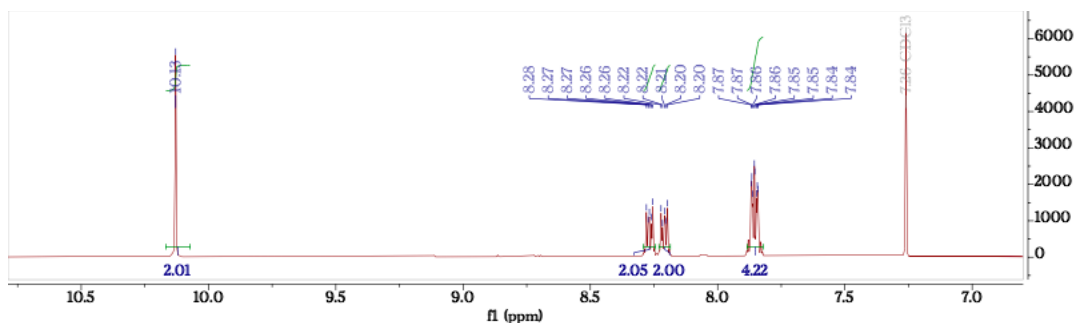


2-(quinolin-2-yl)quinoxaline (**L4**) was synthesized by a reported procedure in 85% yield.⁸ (400 MHz, CDCl₃): δ 10.23 (s, 1H), 8.75 (d, 1H), 8.36 (d, 1H), 8.27 (d, 1H), 8.20 (m, 2H), 7.90 (d, 1H), 7.81 (m, 3H), 7.62 (dd, 1H).

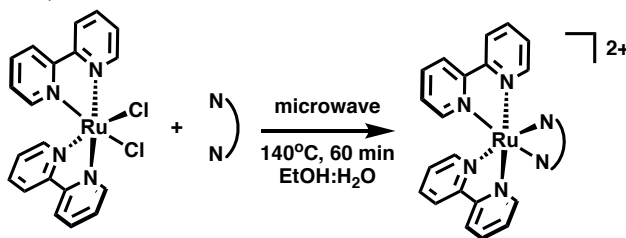


2,2'-biquinoxaline (**L5**). This ligand was synthesized by a modified reported procedure by first forming the hydrochloride salt of quinoxaline followed by homocoupling.⁹ Quinoxaline (6.76 g, 51.9 mmol) was dissolved in 100 mL THF. The solution was cooled to 0°C and 5 mL of concentrated HCl was added dropwise. Immediately an off-white solid began to form. Once all of the HCl was added, the solution was stirred at 0°C for 10 min, the solid was filtered, washed with cold THF, air dried, and collected (6.22g, 72%). Quinoxaline hydrochloride (6.22 g, 37.3 mmol) was dissolved in 48 mL dry dimethylformamide. The solution was degassed with N₂ gas for 10 min at which point N,N'-dimethylaniline (4.81 mL, 37.9 mmol) was added causing the solid to dissolve and the solution to turn dark. The reaction was heated to 140°C and stirred at that temperature for 1.5 hrs. The solution was cooled and 400 mL of 2 M ammonium hydroxide solution was added generating a dark purple precipitate. The solid was filtered and washed with ~ 200 mL methanol. The dark purple solid was redissolved in ~450 mL chloroform and stirred with 1.7 g of charcoal overnight. The solution was filtered and the filtrate taken to dryness to reveal the product as a light red solid (1.0 g, 10%). This product was used without further purification. R_f (3:1 petroleum ether:ethyl acetate) 0.7. ¹H NMR (400 MHz, CDCl₃): δ 10.13 (s, 2H), 8.26 (m, 2H), 8.21 (m, 2H), 7.85 (m, 4H).

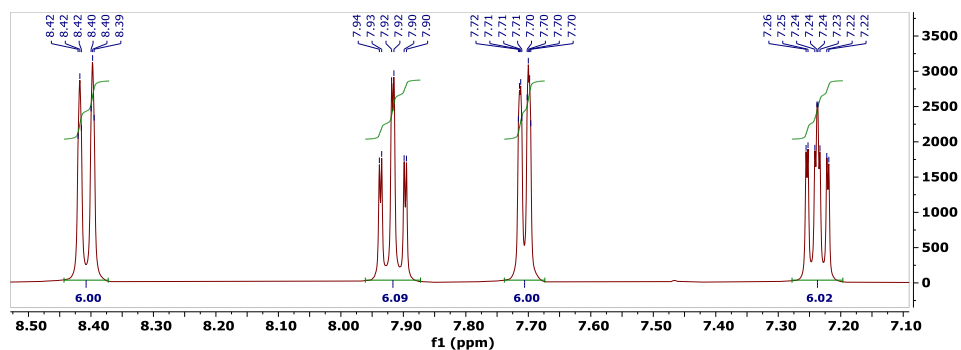




Complex Synthesis. General Procedure. Ru(bpy)₂Cl₂ (0.15 g, 0.31 mmol) and N-N ligand (0.31 mmol) were dissolved in 20 mL of 1:1 EtOH:H₂O in an 80 mL microwave flask. The solution was heated with stirring to 140°C for 60 min. In general, reaction progress can be followed by UV-Vis spectroscopy. The reaction mixture was cooled, filtered, and the filtrate was taken to dryness on a rotary evaporator. The crude product was purified by size exclusion chromatography (Sorbadox, S-25 Fine), like fractions by UV-Vis spectroscopy were combined, and the solvent was removed by rotary evaporation. The solid was triturated with ether, filtered, washed with ether, and collected.

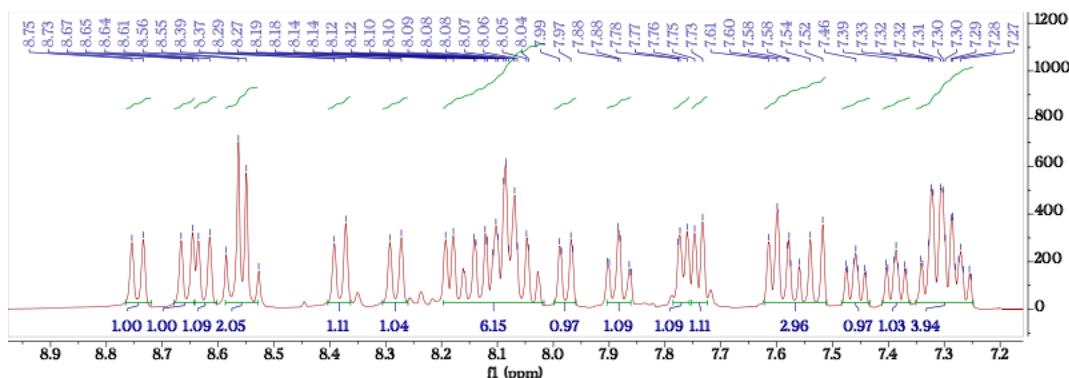


[Ru(bpy)₃]Cl₂ (1). This complex was isolated as a bright orange solid and characterization matches that of previously reported (182 mg, 92%).⁸ ¹H NMR (400 MHz, D₂O) δ 8.41 (d, J = 8.2 Hz, 6H), 7.92 (td, J = 7.9, 1.5 Hz, 6H), 7.71 (dd, J = 5.7, 0.8 Hz, 6H), 7.24 (ddd, J = 7.6, 5.6, 1.3 Hz, 6H). UV-vis in H₂O, λ_{max}, nm (ε, M⁻¹, cm⁻¹) 242 (21300), 287 (69090), 354 (5200), 422 (8500), 456 (10450). HR-ESI-MS: m/z = 285.0538 (calculated for C₂₀H₁₆N₄Ru [M - 2 Cl]²⁺ = 285.055). Anal. Found (Calc) for pentahydrate C₃₀H₃₄Cl₂N₆O₅Ru: C 48.98 (49.32), H 4.65 (4.69), N 11.21 (11.50).

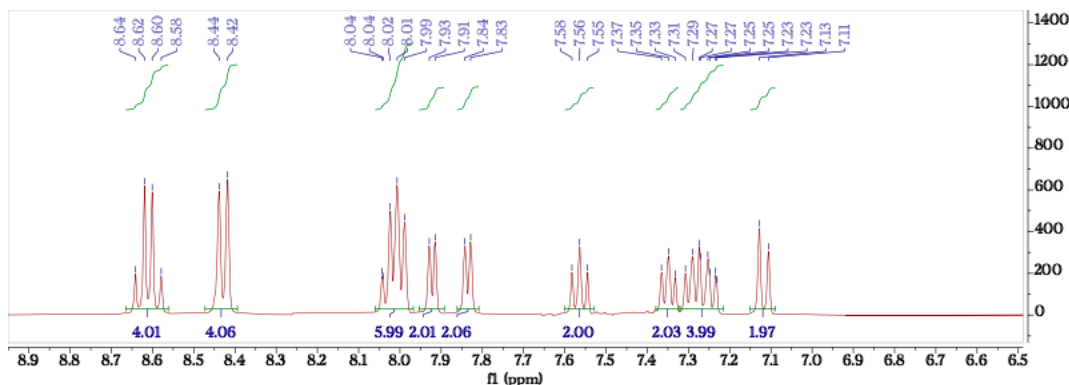


[Ru(bpy)₂(L2)]Cl₂ (2). This complex was isolated as a dark orange solid (0.078 g, 36%). ¹H NMR (400 MHz, D₂O): δ 8.74 (d, 1H), 8.66 (d, 1H), 8.62 (d, 1H), 8.56 (m, 2H), 8.38 (d, 1H), 8.28 (d, 1H), 8.08 (m, 6H), 7.98 (d, 1H), 7.88 (dd, 1H), 7.77 (d, 1H), 7.74 (d, 1H), 7.56 (m, 3H), 7.46 (dd, 1H), 7.39 (dd, 1H), 7.31 (m, 4H). UV-vis in H₂O, λ_{max}, nm (ε, M⁻¹, cm⁻¹) 238 (28000), 278 (38900), 351

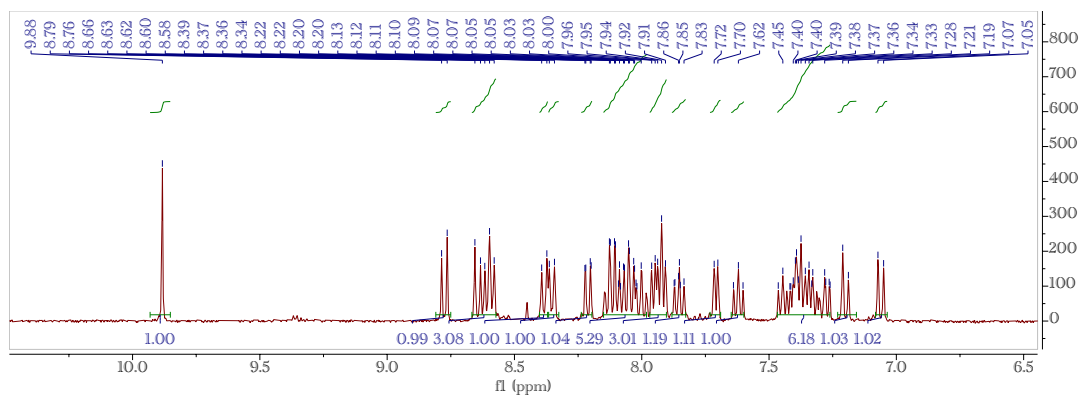
(7780), 449 (8310), 489 (6770). HR-ESI-MS: $m/z = 310.0692$ (calculated for $C_{34}H_{26}N_6Ru [M - 2 Cl^-]^{2+} = 310.065$). Anal. Found (Calc) for pentahydrate $C_{34}H_{36}Cl_2N_6O_5Ru$: C 52.47 (52.31), H 4.46 (4.65), N 10.69 (10.77).



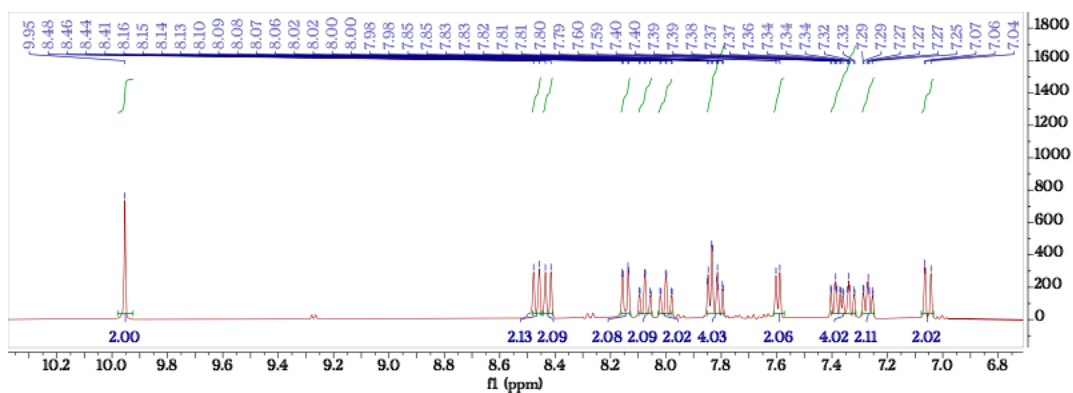
[Ru(bpy)₂(L3)]Cl₂ (3). This complex was isolated as a dark red solid (0.084 g, 37%). ¹H NMR (400 MHz, D₂O): δ 8.61 (dd, 4H), 8.43 (d, 4H), 8.02 (m, 6H), 7.92 (d, 2H), 7.83 (d, 2H), 7.56 (dd, 2H), 7.35 (d, 2H), 7.27 (m, 4H), 7.12 (d, 2H). UV-vis in H₂O, λ_{max} , nm (ϵ , M⁻¹, cm⁻¹) 265 (31100), 285 (34400), 352 (12500), 378 (9780), 439 (4200), 527 (4270). HR-ESI-MS: $m/z = 335.0704$ (calculated for $C_{37}H_{27}N_6Ru [M - 2 Cl^-]^{2+} = 335.070$). Anal. Found (Calc) for pentahydrate $C_{38}H_{38}Cl_2N_6O_5Ru$: C 55.5 (54.94), H 4.42 (4.61), N 10.22 (10.12).



[Ru(bpy)₂(L4)]Cl₂ (4). This complex was isolated as a purple solid (0.206 g, 90%). ¹H NMR (400 MHz, D₂O): δ 9.88 (s, 1H), 8.77 (d, 1H), 8.62 (m, 3H), 8.38 (d, 1H), 8.35 (d, 1H), 8.21 (dd, 1H), 8.05 (m, 5H), 7.93 (m, 3H), 7.85 (dd, 1H), 7.71 (d, 1H), 7.62 (dd, 1H), 7.37 (m, 6H), 7.21 (d, 1H), 7.06 (d, 1H). λ_{max} , nm (ϵ , M⁻¹, cm⁻¹) 255 (22100), 273 (31200), 286 (34500), 359 (12900), 393 (11800), 434 (5100), 553 (5170). HR-ESI-MS: $m/z = 335.5692$ (calculated for $C_{37}H_{27}N_7Ru [M - 2 Cl^-]^{2+} = 335.568$). Anal. Found (Calc) for pentahydrate $C_{38}H_{37}Cl_2N_7O_5Ru$: C 53.62 (53.43), H 4.30 (4.48), N 11.68 (11.79).



[Ru(bpy)₂(L5)]Cl₂ (5). This complex was isolated a dark purple solid (0.11 g, 48%). ¹H NMR (400 MHz, D₂O): δ 9.95 (s, 2H), 8.47 (d, 2H), 8.43 (d, 2H), 8.15 (d, 2H), 8.07 (dd, 2H), 8.00 (dd, 2H), 7.82 (m, 4H), 7.59 (d, 2H), 7.36 (m, 4H), 7.27 (dd, 2H), 7.05 (d, 2H). UV-vis in H₂O, λ_{max}, nm (ε, M⁻¹, cm⁻¹) 254 (30600), 280 (53000), 386 (22400), 405 (21800), 565 (7705). HR-ESI-MS: m/z = 336.0665 (calculated for C₃₆H₂₆N₈Ru [M – 2 Cl]²⁺ = 336.065). Anal. Found (Calc) for pentahydrate C₃₆H₃₆Cl₂N₈O₅Ru: C 52.41 (51.98), H 4.08 (4.36), N 13.25 (13.46).



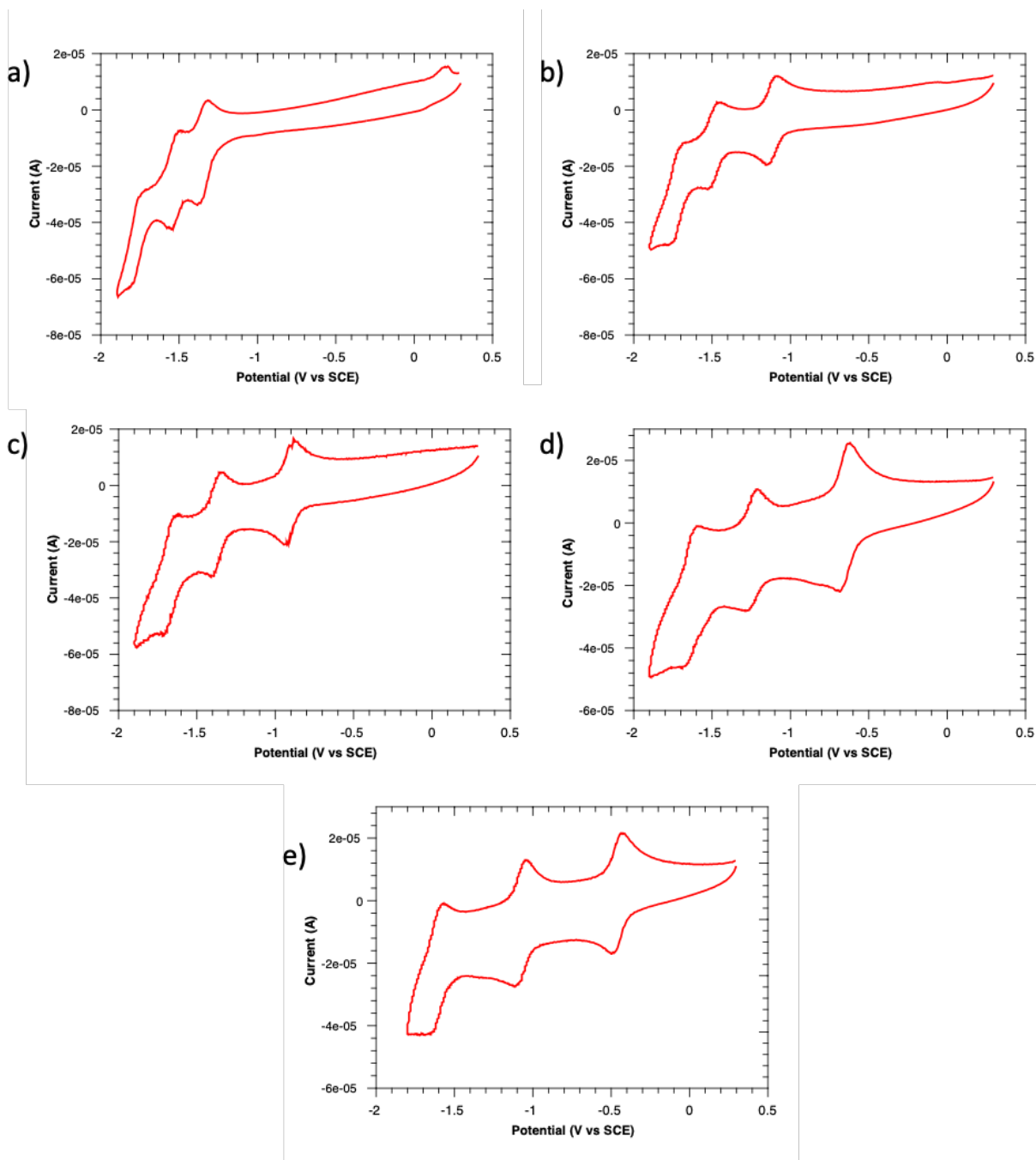


Figure S1. Cyclic voltammograms acquired at 100 mV/s for 1 mM solutions of **1** (a), **2** (b), **3** (c), **4** (d), and **5** (e) in Ar deaerated CH_3CN with 0.1 M TBAPF_6 supporting electrolyte. GC working electrode, graphite rod counter electrode, and Ag/AgNO_3 reference electrode (0.01 M AgNO_3 with 0.1 M TBAPF_6 in CH_3CN). Values were adjusted to agree with literature values for $[\text{Ru}(\text{bpy})_3]^{3+/2+}$ at 1.29 V vs SCE.³

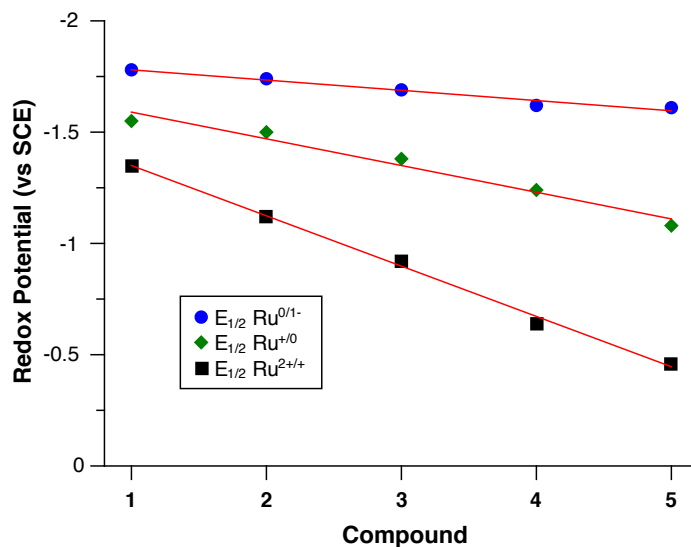


Figure S2. Reduction potentials for compounds **1** – **5** in CH_3CN deaerated with Ar for 10 min, 1 mM in complex and 0.1 M TBAPF_6 supporting electrolyte. GC working electrode, graphite rod counter electrode, and Ag/AgNO_3 (0.01 M AgNO_3 with 0.1 M TBAPF_6 in CH_3CN) reference (values were adjusted to agree with literature values for $[\text{Ru}(\text{bpy})_3]^{3+/2+}$ at 1.29 V vs SCE).¹⁻⁴ $E_{1/2}$ values from differential pulse voltammetry.



Figure S3. Photolysis setup used to study photoinduced ligand ejection processes from complexes. The samples were dissolved in 3 mL of deionized water and illuminated with a (left) Kessil PR160 lamp (467 nm, 120 mW/cm^2 at 5 cm) or (right) GLORIOUS-LITE 30W LED (240W halogen equivalent), 3000 LM broad spectrum white light that was held 5 cm away from the sample with constant stirring.

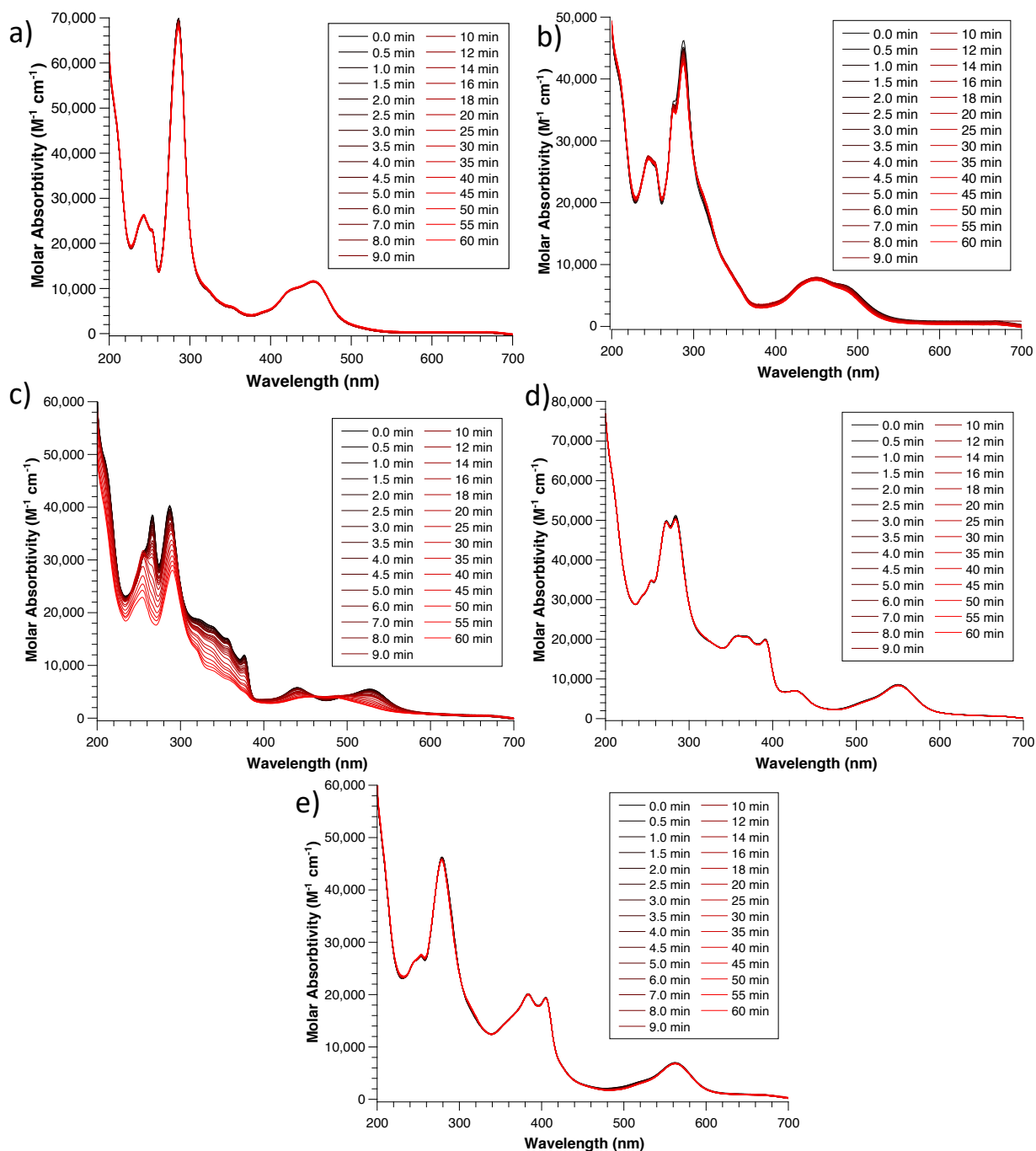


Figure S4. Absorption spectra of complexes **1** (a), **2** (b), **3** (c), **4** (d), and **5** (e) in 3 mL H₂O monitored over time during irradiation with light from a Kessil PR160 (467 nm, 120 mW/cm² at 5 cm). Light intensity was adjusted to correct for varying molar absorptivities at 467 nm 25% for **1**, 25% for **2**, 75% for **3**, 100% for **4**, and 100% for **5**.

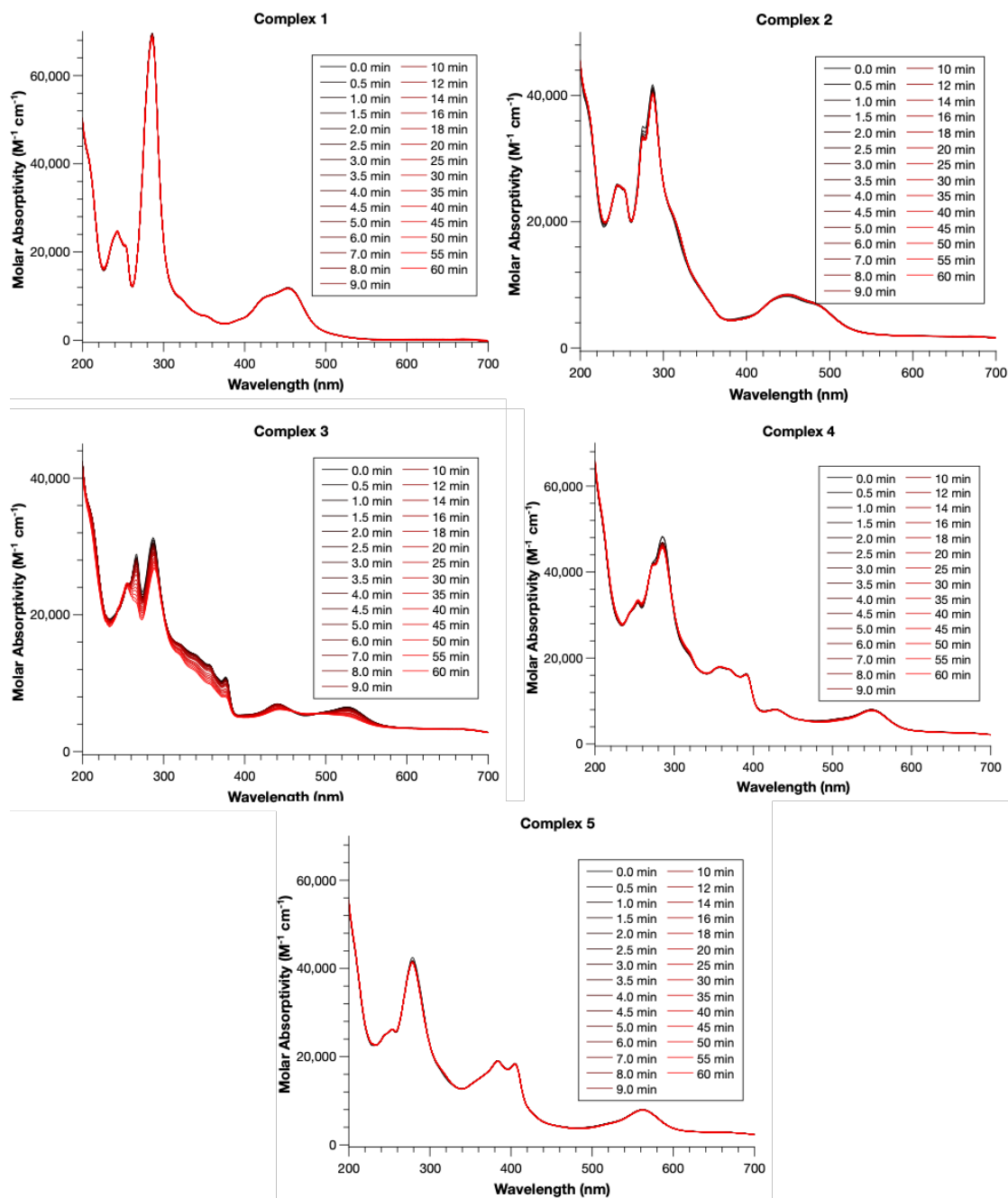


Figure S5. Absorption spectra of complexes **1** - **5** in 3 mL H₂O monitored over time during irradiation with light from a GLORIOUS-LITE 30W LED (240W halogen equivalent), 3000 LM broad spectrum white light placed 5 cm away from the sample. First order rates constants for k_{pld} were **1** ($\ll 10^{-6} s^{-1}$) < **2** ($3.4 \times 10^{-6} s^{-1}$) < **3** ($6.4 \times 10^{-5} s^{-1}$).

Table S1. Molar absorption of each complex at 467 nm and the light intensity used on the Kessil PR160 lamp to account for these differences.

Compound	Molar Abs. at 467nm	Light intensity (%)
1	9188	25
2	7039	25
3	3078	75
4	2444	100
5	2193	100

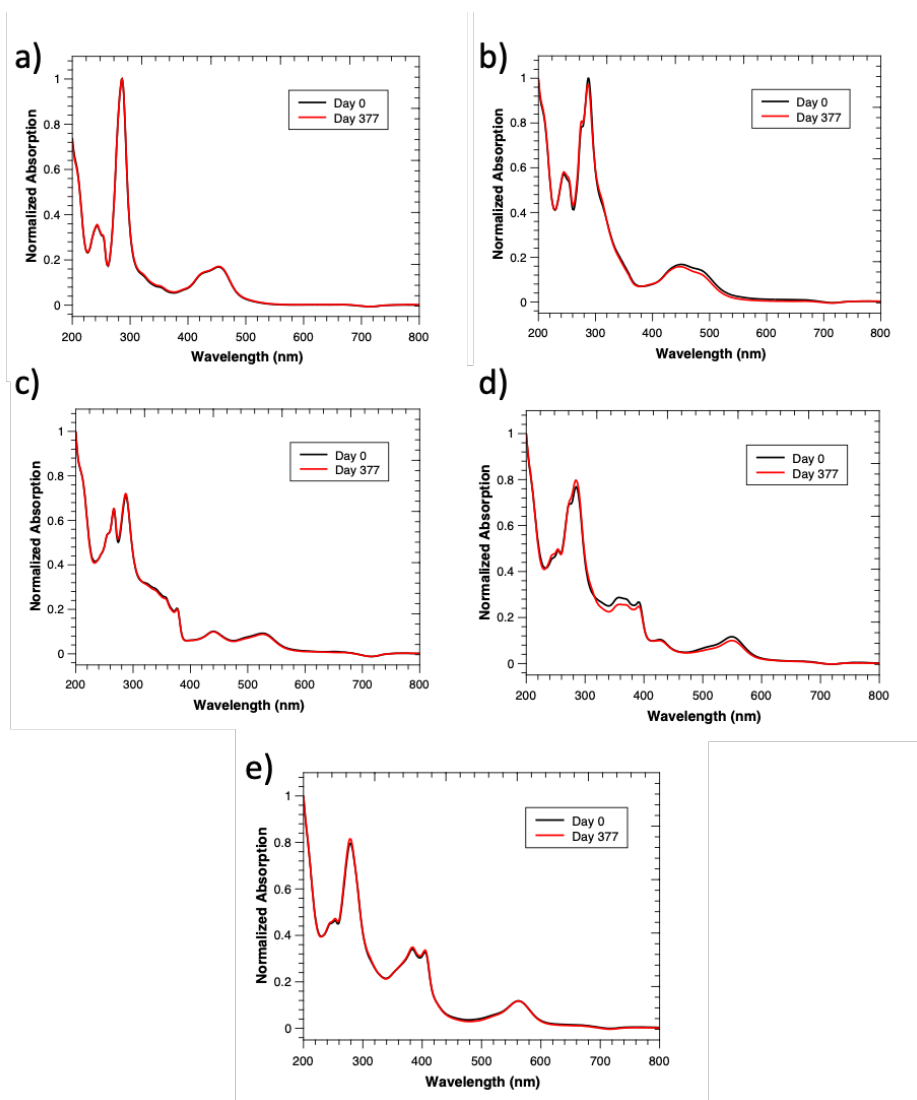


Figure S5. Absorption spectra of complexes **1** (a), **2** (b), **3** (c), **4** (d), and **5** (e) in H₂O initially (black) and 377 days later being stored in the dark.

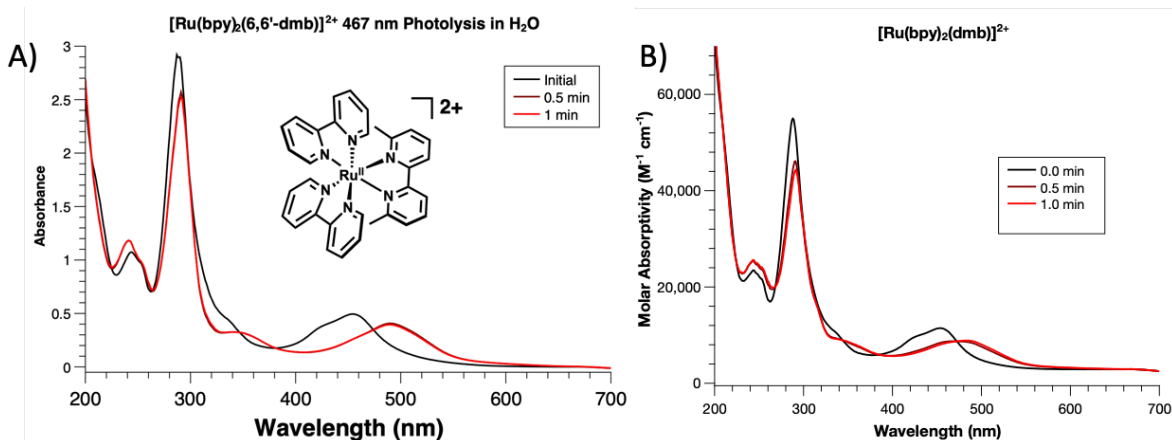


Figure S6. Absorption spectra of $[\text{Ru}(\text{bpy})_2(6,6'\text{-dmb})]^{2+}$ in 3 mL H_2O monitored over time during irradiation with light from a (A) Kessil PR160 (467 nm, $120 \text{ mW}/\text{cm}^2$ at 5 cm) set to 25% intensity and a (B) GLORIOUS-LITE 30W LED (240W halogen equivalent), 3000 LM broad spectrum white light placed 5 cm away from the sample.

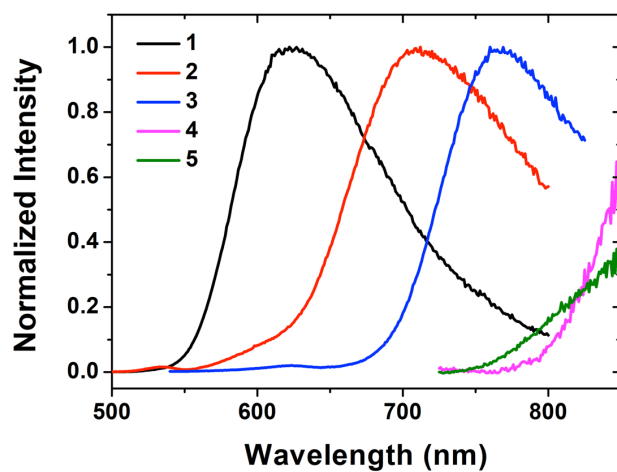


Figure S7. Normalized emission spectra of **1-5** in N_2 deaerated H_2O ($\lambda_{\text{ex}} = 445 \text{ nm}$).

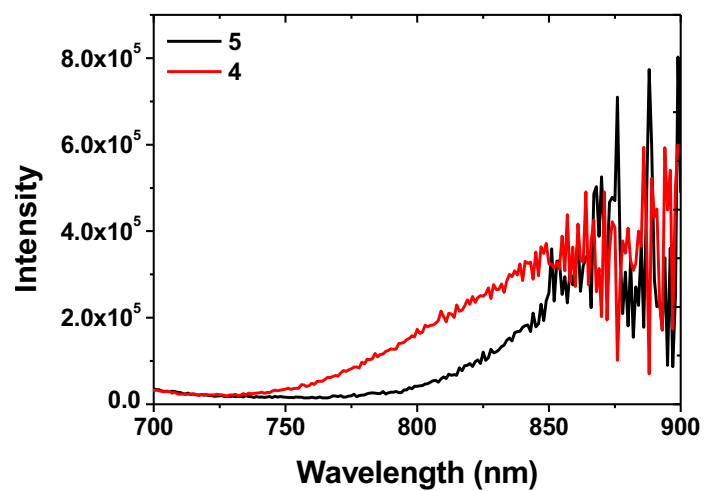


Figure S8. Emission spectra of **4** and **5** in N₂ deaerated H₂O ($\lambda_{ex} = 550$ nm).

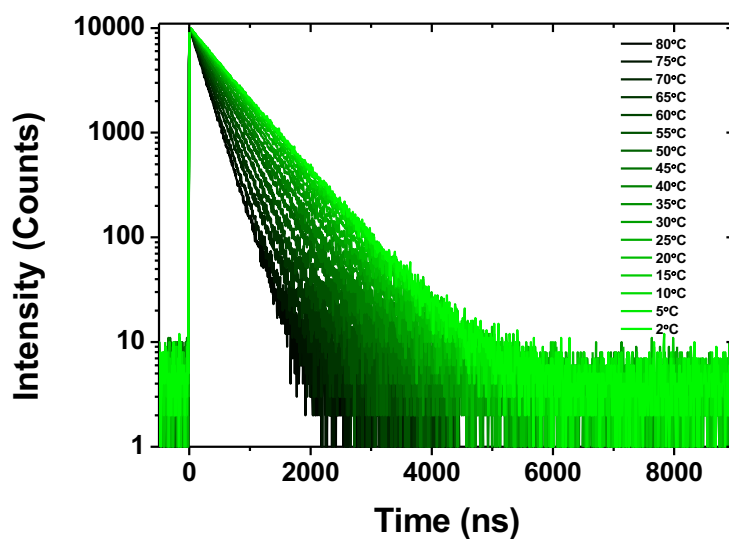


Figure S9. Emission decays for **1** in N₂ deaerated H₂O ($\lambda_{ex} = 405$ nm, $\lambda_{em} =$ emission maximum).

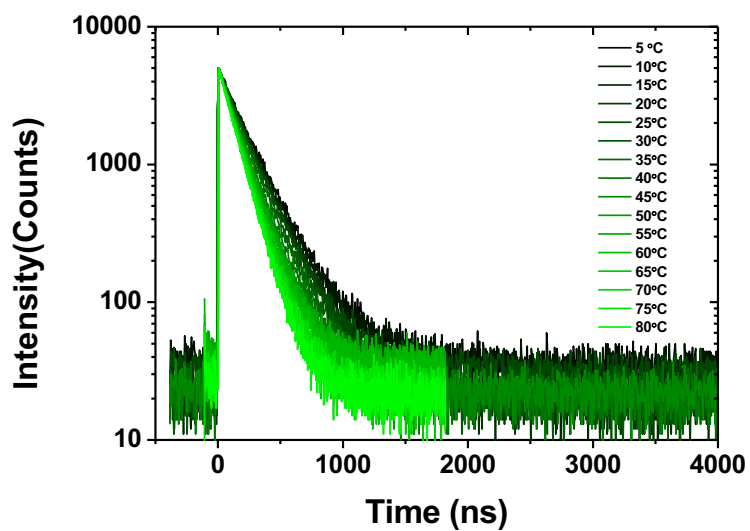


Figure S10. Emission decays for **2** in N₂ deaerated H₂O ($\lambda_{\text{ex}} = 405 \text{ nm}$, $\lambda_{\text{em}} = \text{emission maximum}$).

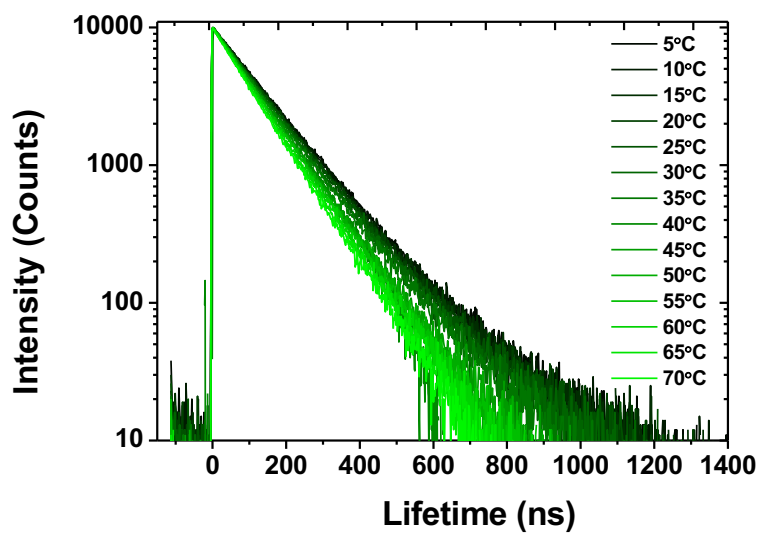


Figure S11. Emission decays for **3** in N₂ deaerated H₂O ($\lambda_{\text{ex}} = 405 \text{ nm}$, $\lambda_{\text{em}} = \text{emission maximum}$).

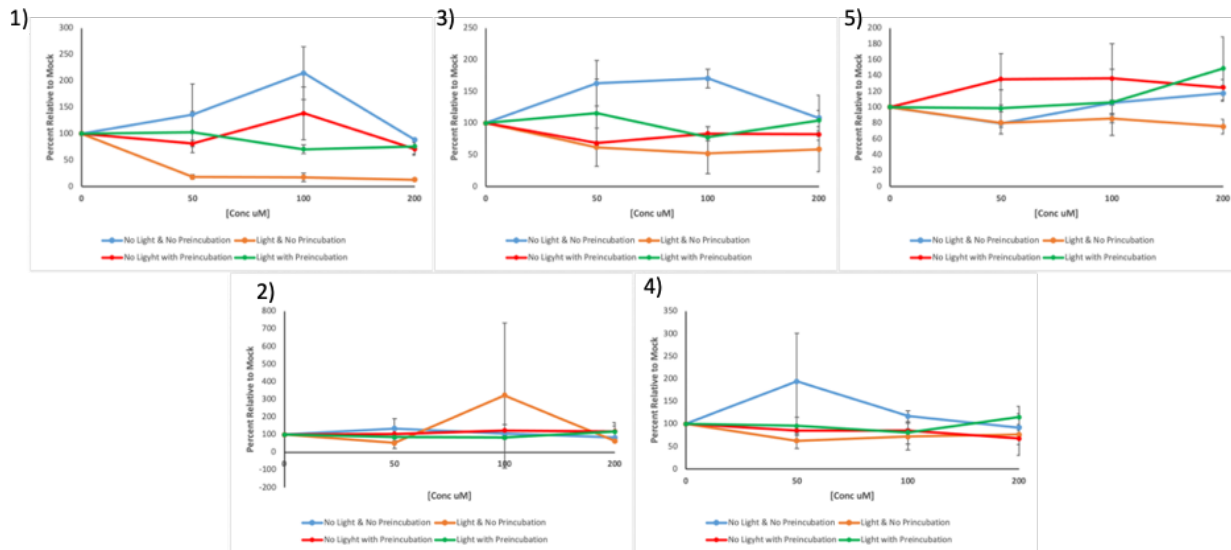


Figure S12. Cell viability assays as measured by the function of MTT dye reduction following incubation with complexes 1 – 5. Viability measurements were conducted in triplicate for each condition.

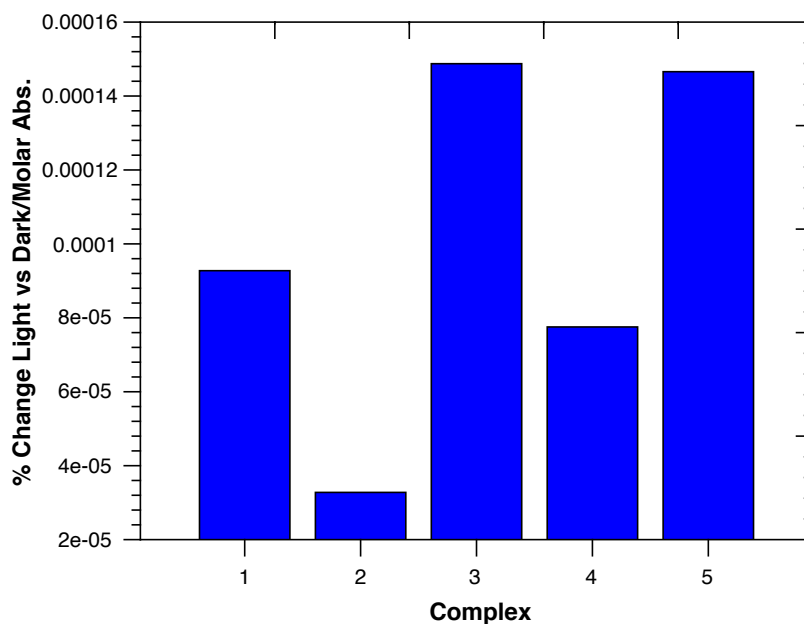


Figure S13. Percent change in cell viability of light vs dark divided by the molar absorptivity at 467 nm for each complex.

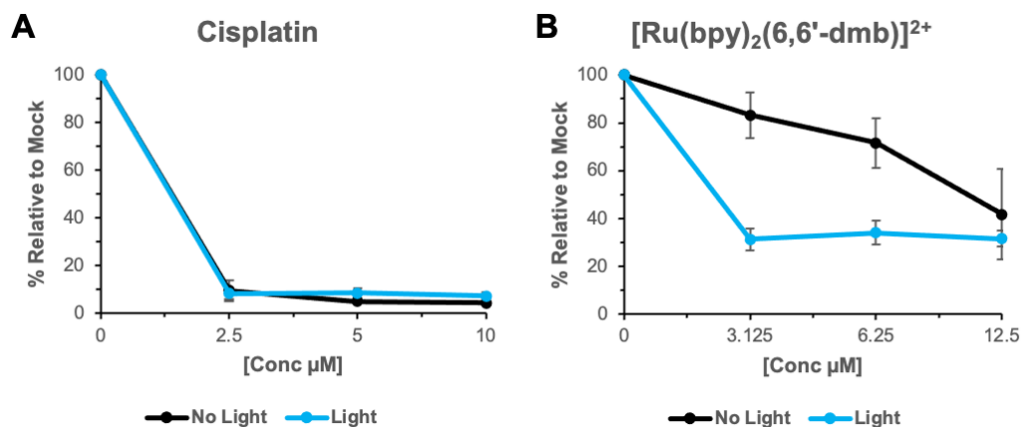


Figure S14. Cell viability assays as measure by the function of MTT dye reduction following incubation with positive control compounds cisplatin and [Ru(bpy)₂(6,6'-dmb)]²⁺. As expected, both compounds display significant cytotoxicity against the HEK293T cell line. Cytotoxicity of the [Ru(bpy)₂(6,6'-dmb)]²⁺ displays a dependency on irradiation, as described previously¹⁰, whereas irradiation has no effect on the cytotoxicity of cisplatin.

References

1. Thompson, D. W.; Ito, A.; Meyer, T. J., [Ru(bpy)₃]²⁺* and other remarkable metal-to-ligand charge transfer (MLCT) excited states. *Pure and Applied Chemistry* **2013**, *85* (7), 1257-1305.
2. Anderson, P. A.; Keene, F. R.; Meyer, T. J.; Moss, J. A.; Strouse, G. F.; Treadway, J. A., Manipulating the properties of MLCT excited states. *Journal of the Chemical Society, Dalton Transactions: Inorganic Chemistry (1972-1999)* **2002**, (20), 3820-3831.
3. Lever, A. B. P., Electrochemical parametrization of metal complex redox potentials, using the ruthenium(III)/ruthenium(II) couple to generate a ligand electrochemical series. *Inorganic Chemistry* **1990**, *29* (6), 1271-85.
4. Gu, J.; Chen, J.; Schmehl, R. H., Using Intramolecular Energy Transfer to Transform non-Photoactive, Visible-Light-Absorbing Chromophores into Sensitizers for Photoredox Reactions. *Journal of the American Chemical Society* **2010**, *132* (21), 7338-7346.
5. Fast, Olivia G.; Gentry, B.; Strouth, L.; Niece, Madison B.; Beckford, Floyd A.; Shell, Steven M., Polynuclear ruthenium organometallic compounds induce DNA damage in human cells identified by the nucleotide excision repair factor XPC. *Bioscience Reports* **2019**, *39* (7).
6. Lawrence, M. L.; Shell, S. M.; Beckford, F. A., Binuclear manganese-iron complexes containing ferrocenyl thiosemicarbazones: Biological activity and carbon monoxide-releasing properties. *Inorganica Chimica Acta* **2020**, *507*, 119548.
7. Norris, M. R.; Concepcion, J. J.; Glasson, C. R. K.; Fang, Z.; Lapidés, A. M.; Ashford, D. L.; Templeton, J. L.; Meyer, T. J., Synthesis of Phosphonic Acid-Derivatized Bipyridine Ligands and Their Ruthenium Complexes. *Inorganic Chemistry* **2013**, *52* (21), 12492-12501.
8. Ashford, D. L.; Glasson, C. R. K.; Norris, M. R.; Hanson, K.; Concepcion, J. J.; Keinan, S.; Brennaman, M. K.; Templeton, J. L.; Meyer, T. J., Controlling Ground and Excited State

Properties through Ligand Changes in Ruthenium Polypyridyl Complexes. *Inorg Chem* **2014**, *53* (11), 5637-5646.

9. Leblanc, N.; Sproules, S.; Fink, K.; Sanguinet, L.; Alévêque, O.; Levillain, E.; Rosa, P.; Powell, A. K., A fascinating multifaceted redox-active chelating ligand: introducing the N,N'-dimethyl-3,3'-biquinoxalinium "methylbiquinoxen" platform. *Chemical Science* **2016**, *7* (6), 3820-3828.

10. Howerton, B. S.; Heidary, D. K.; Glazer, E. C., Strained Ruthenium Complexes Are Potent Light-Activated Anticancer Agents. *Journal of the American Chemical Society* **2012**, *134* (20), 8324-8327.